Magnetic domain structure and magnetization reversal in amorphous microwires with circular anisotropy: A micromagnetic approach

I. Betancourt,[1,a)] G. Hrkac,[2] and T. Schrefl[2,3]
[1]*Departamento de Materiales Metálicos y Cerámicos, Instituto de Investigaciones en Materiales, Universidad Nacional Autónoma de México, México D.F. 04510, Mexico*
[2]*Department of Engineering Materials, University of Sheffield, Mappin St, Sheffield S1 3JD, United Kingdom*
[3]*St. Pölten University of Applied Sciences, 3100 St. Pölten, Austria*

(Received 27 January 2010; accepted 9 November 2010; published online 4 January 2011)

In this work we present a numerical investigation on the magnetic domain formation and magnetization reversal mechanism in submillimeter (250 μm length) amorphous microwires with negative magnetostriction by means of micromagnetic calculations. The formation of circular magnetic domains surrounding an axially, multidomain-oriented central nucleus was observed for the micromagnetic model representing the amorphous microwire. The magnetization reversal described by micromagnetic computations is consistent with a combined nucleation-propagation-rotational mechanism for the magnetization reversal after the saturated state. © *2011 American Institute of Physics*. [doi:10.1063/1.3525564]

I. INTRODUCTION

Amorphous alloys having cylindrical geometry are among the softest magnetic materials currently used for technological applications. In particular, Iron-based and Co-based amorphous glass coated microwires obtained by means of the Taylor–Ulitovsky technique (which allows the production of very large fibers having diameters ranging from 2 to 40 μm of metallic core surrounded by a glass outer shell of variable thickness within the range 2–30 μm, typically[1–4]) have been subject of active research due to their very soft magnetic character including magnetic bistability, i.e., a very well defined rectangular *M-H* loop afforded by a single Barkhausen jump. Because of the absence of crystalline anisotropy in these systems, the domain structure and consequently, the hysteresis properties, are a resultant of shape anisotropy and magnetoelastic energy. The magnetoelastic properties are determined by the complex quenched-in stresses configuration arising from the casting process, especially from the strong thermal gradient between the core and the outer region of the wire, together with the saturation magnetostriction coefficient, λ_s. This λ_s determines to a large extent the peculiar magnetic domain configuration which characterize this kind of magnetic microwires: an inner zone with magnetic axial orientation surrounded by a sheath of perpendicular magnetization with either radial (characteristic of by Fe-based microwires with large positive λ_s) or circular orientation (typical of Co-based and CoFe-based microwires with negative λ_s).[1–4] In this work we present a numerical investigation of the magnetic domain formation and magnetization reversal mechanism in very short amorphous microwires with circular anisotropy by means of the continuum theory of micromagnetism.

[a)]Electronic mail: israelb@iim.unam.mx.

II. NUMERICAL METHOD

Micromagnetic calculations are based on the dynamic magnetization description given by the Landau–Lifshitz–Gilbert (LLG) equation of motion

$$\frac{\partial \mathbf{M}}{\partial t} = -\gamma' \mathbf{M} \times \mathbf{H}_{\text{eff}} - \frac{\alpha \gamma'}{M_s} \mathbf{M} \times (\mathbf{M} \times \mathbf{H}_{\text{eff}}), \quad (1)$$

where α is the dimensionless damping constant, γ is the electron gyromagnetic ratio, and $\gamma' = \gamma/(1+\alpha^2)$. The effective field $\mathbf{H}_{\text{eff}}$ is composed of the anisotropy field $\mathbf{H}_{\text{ani}}$, the exchange contribution $\mathbf{H}_{\text{ex}}$, the applied field $\mathbf{H}_a$ and the magnetostatic field $\mathbf{H}_M$.[5] In order to use Eq. (1) for calculating the equilibrium magnetization in a cylindrical model representing an amorphous microwire, the microwire model is discretized into tetrahedral finite elements according to the Ritz–Galerkin weak formulation.[5,6] For each node of the finite element mesh, a magnetic moment vector, and a magnetic scalar potential is defined. The magnetic scalar potential follows from the magnetostatic boundary value problem. Instead of extending the finite element mesh over a larger region outside the magnet, the boundary element method allows to treat the condition that the potential decays as 1/r with distance.[7,8] The space discretization of the LLG equation leads to a system of ordinary differential equations for the magnetic moment at the nodes of the finite element mesh. The equations are coupled by the exchange field and by the magnetostatic field and are solved by means of a time-integration technique, for which we use an implicit time-integration scheme with automatic time step control.[9,10]

The amorphous microwire model considered in this study consisted of a solid cylinder of 20 μm diameter and 250 μm length with its longitudinal axis oriented along the z direction. For this microwire model we describe the magnetostriction by an effective magnetic anisotropy constant K_{eff}. This K_{eff} results from the magnetoelastic coupling between the internal stresses induced during the wire's fabrication

process and the sign of λ_s, which in turn is determined by the chemical composition.[1–4] For real amorphous microwires two main kinds of stresses are identified (a) axial stress due to the cooling process and (b) radial stress caused by the difference in thermal expansion coefficients between the metallic nucleus and the glass coating.[1–4,11] The internal stress variations in amorphous microwires follow a rather complex distribution with axial, circular, and radial components changing rapidly from positive (at the axial zone) to negative (at the surrounding shell) including maximum values at half the radius as well as on the wire edges.[12,13] Even zero stress value is expected at the very microwire center.[12,13] For the present micromagnetic model, the effective anisotropy constant K_{eff} was set on as 500 J/m^3 for the whole model with the following distribution: longitudinal direction in an inner cylindrical core of radius $R_c=8.5$ μm and circumferential orientation in a surrounding external sheath of 1.5 μm thickness. The circular anisotropy is a consequence of the radial distribution of mechanical stresses frozen during the fabrication process, while for the internal core, the resultant stress variation with longitudinal orientation leads to axial easy direction reinforced by shape anisotropy. In addition, at the very center of the microwire, the axial orientation is also promoted by exchange interactions, which are energetically more favored than the circular direction of the external surface.

On the other hand, the remaining intrinsic magnetic properties assigned to this model were taken from experimental reports concerning amorphous CoFe microwires with negative λ_s:[3,4] saturation polarization $\mu_0 M_s=0.8$ T, exchange constant $A=1\times10^{-11}$ J/m and damping constant α of 0.01. The small α value used is consistent with a homogenous amorphous structure, as it has been experimentally reported in Fe–B–Y similar amorphous alloys.[14] The ratio $R_c/R_w=0.85$ of the central radius R_c to the total wire radius R_w was fixed according to experimental reports for amorphous microwires of equivalent composition and diameter.[11]

A fundamental issue in this micromagnetic study is the exchange length L_{ex} for amorphous alloys, which determines to a large extent the viability of the numerical computations. According to the Random Anisotropy Model, L_{ex} for amorphous alloys can be established as follows:[4,15–17]

$$L_{ex}=\frac{16A^2}{9K_l^2d^3}, \tag{2}$$

where A stands for the exchange constant and K_l for the local anisotropy (i.e., the magnetic anisotropy of the short-range-order, local atom configurations characteristic of the amorphous structure), while d corresponds to the structural correlation length. For amorphous alloys, $A\sim10^{-11}$ J/m and $K_l\sim10^4-10^5$ J/m^3,[15–17] whereas d can be taken as being of the interatomic distance order, i.e., $d\sim10^{-9}$ m.[15,16] Thus, by using these A, K_l, and d parameters in Eq. (2), we have $L_{ex}\approx10$ μm. For this work we use $L_{ex}=2.5$ μm. This exchange length affords the discretization of the microsized model cylinders described above with a mesh containing a number of finite elements around 400 000, well fitted for finite time computation purposes.

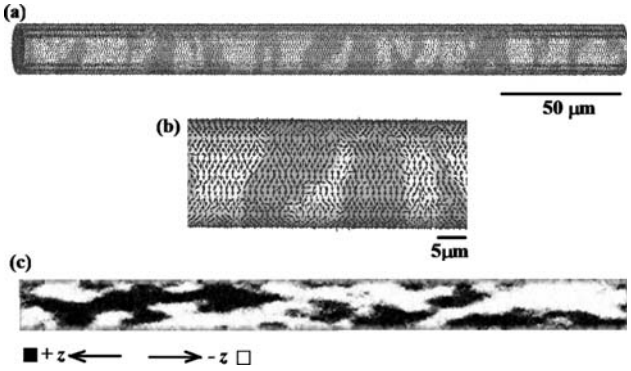

FIG. 1. (Color online) (a) Surface equilibrium magnetization distribution for the micromagnetic model, (b) magnification of middle portion of the microwire model showing the magnetization distribution in detail, and (c) corresponding transverse y-z profile for the entire model.

III. RESULTS

Equilibrium magnetic states were calculated by integrating Eq. (1) for 300 ns, whereby the initial configuration was a random magnetization. The corresponding equilibrium magnetization distribution is shown in Fig. 1(a), for which the formation of circular-like magnetic domains of alternate orientation on the cylinder surface is manifested by the magnetization representation by means of arrows. The amplification of the central microwire model portion included in Fig. 1(b) makes evident the formation of zones with such distinctive circular magnetization directions. Additionally, the magnetic domain configuration of the microwire inner axial zone is shown in Fig. 1(c) as a transverse y-z profile for which a longitudinal oriented magnetization is observed with a multidomain structure along $\pm z$ directions as indicated by the contrast code used for this zone: black for $+z$ direction and white for $-z$ orientation.

On the other hand, the magnetization M-H curve resulting from the application of an external field H_z from +0.1 to −0.1 T (i.e., half loop) along the $\pm z$ direction is exhibited in Fig. 2, for which a saturated state is observed from $H_z=0.1$ T up to $H_z=0.03$ T, together with a small coercive field H_c of 0.0018 T and a relative remanence magnetization $M_r/M_s=0.18$ T (Fig. 2, inset). In addition, the M-H plot

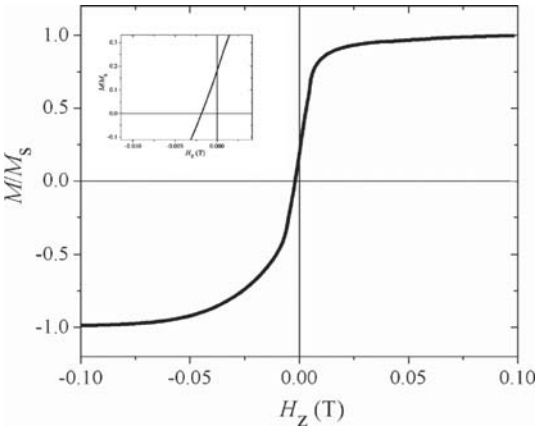

FIG. 2. Magnetization M-H curve for the amorphous microwire model. The external field is applied along the $\pm z$ direction.

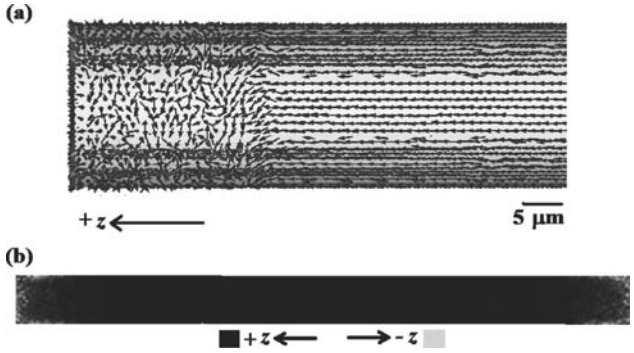

FIG. 3. Magnetization reversal process for the amorphous microwire model showing (a) nucleation of surface circular-like domains nearby the model ends for $H_z=0.03$ T (magnified detail for the wire left edge) and (b) the corresponding central y-z profile for the entire axial zone exhibiting an almost saturated state along $+z$ with few misaligned areas at both microwires ends.

present a nonsymmetric vertical aspect which can be associated with the magnetization reversal mechanism identified as comprising nucleation and propagation of circular-like surface domains and magnetic moment rotation. Specifically, for the negative $-H_z$, $-M$ section, the curve exhibits a change in slope for $H_z<-0.0075$ T, which coincides with the onset of the rotational process toward the negative saturation state, as it is described in detail for the whole magnetization reversal process in Figs. 3–6 as follows: on the microwire surface the nucleation of circular-like domains at the wire edges begins at $H_z=0.03$ T [Fig. 3(a)], while at the axial zone [Fig. 3(b)] an almost saturated state along $+z$ is observed by the contrast code (black $+z$; light-gray $-z$) corresponding to a central y-z profile, which includes few misaligned areas at both microwires ends (indicated by dark-gray color). Further reduction in H_z(=0.0050 T) favors the formation of two circular domains of opposite orientation on the microwire surface, as shown in detail in Fig. 4(a); while at the central zone the majority axially oriented magnetization is still present [Fig. 4(b)]. For the remanent state ($H_z=0$ T), the configuration of a surface helical-like magnetization structure becomes evident as displayed in Fig. 5(a), while the progressive rotation of the central core toward $-z$ direction is manifested by means of increased misaligned zones at both, edges and the middle zones of the microwire [dark-gray and

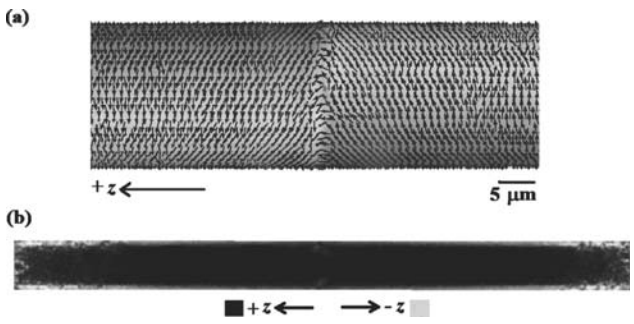

FIG. 4. Magnetization reversal process for the amorphous microwire model showing (a) the formation of two circular domains of opposite orientation at $H_z=0.0050$ T on the model surface (magnified detail for the microwire middle zone) and (b) the corresponding inner part (y-z profile for the entire axial zone) preserves its majority saturated state along $+z$.

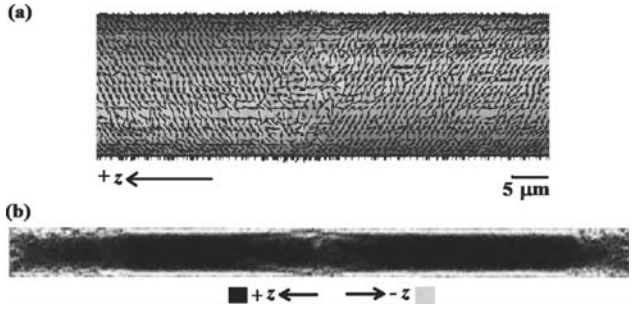

FIG. 5. Magnetization reversal process for the amorphous microwire model showing (a) the remanent state ($H_z=0$ T) for which the surface magnetic configuration consist of a helical-like magnetization structure (magnified detail for the microwire middle zone) and (b) the associated central core (y-z cut for the entire axial zone) exhibiting increased misaligned areas at both, edges and the middle zones of the microwire.

white contrast, Fig. 5(b)]. It is clear that the still predominant axial orientation of the central core contributes significantly to the noticeable relative remanence magnetization observed in the calculated M-H curve (Fig. 2). For the demagnetizing process at $H_z<0$ T, the opposite saturation along $-z$ is progressively developed by means of a rotational mechanism as it is manifested in Fig. 6(a) for the microwire surface at $H_z=-0.0075$ T, which shows an intermediate state of magnetization with random-like orientation reflecting the gradual reorientation of magnetic moments toward $-z$ direction. An equivalent configuration is formed at the axial zone [Fig. 6(b)] for which the contrast code is consistent with a random-like magnetic moment distribution preceding the opposite $-z$ magnetization. The opposite saturation state was observed for $H_z\leq-0.050$ T.

IV. DISCUSSION

The magnetization reversal for this amorphous microwire model with circular anisotropy can be interpreted in terms of the effective magnetic anisotropy K_{eff}, which results from the magnetoelastic coupling between residual stresses induced during the wire's fabrication process and the sign of λ_s.[1–4] The circular direction of K_{eff} for this case provokes the nucleation of circular domains during the reversion of mag-

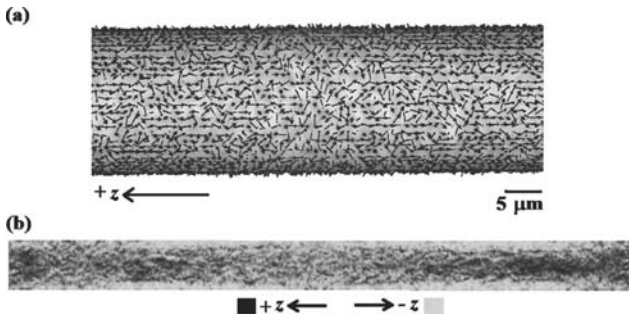

FIG. 6. Magnetization reversal process for the amorphous microwire model showing (a) intermediate state of magnetization at $H_z=-0.0075$ T with surface random-like orientation reflecting the gradual reorientation of magnetic moments toward $-z$ direction (magnified detail for the microwire middle zone) and (b) intermediate state of magnetization at the axial zone (y-z profile for the entire axial zone) exhibiting a random-like magnetic moment distribution preceding the opposite $-z$ magnetization.

netization, thus requiring high external field for rotation toward negative saturation and hence, a rather high coercivity value (H_c=0.0018 T) relative to the coercivity observed for real amorphous wires with typical lengths within the range 5–10 cm and $H_c \sim 0.000\ 05$ T.[18,19] Such large value of coercivity in comparison with experimental data could be originated in the very short length of the microwire model via the shape anisotropy contribution to the anisotropy field $\mathbf{H}_{ani}$ as well as through an increased magnetostatic contribution to the magnetostatic field $\mathbf{H}_M$ for the effective field $\mathbf{H}_{eff}$ in Eq. (1). On the other hand, for experimental amorphous microwires, it is well known the existence of a critical length L_{cr} which ensures the minimization of closure domains at both microwire's ends for the condition $L > L_{cr}$, which affords the formation of a single domain at the central core and hence, the bistable behavior.[4,18–20] For CoFe-based amorphous microwires with circular anisotropy L_{cr}=4 mm,[4,19] which is considerable larger than the length used for our micromagnetic model. Therefore, the multidomain axial structure at the central core observed for the present study is consistent with the magnetic domain distribution expected for short microwires with $L < L_{cr}$.

V. CONCLUSIONS

The formation of circular magnetic domains around a longitudinally oriented multidomain central core was observed for a cylindrical micromagnetic model mimicking amorphous microwires with circular anisotropy. The magnetization reversal described by micromagnetic computations predicts a combined nucleation-propagation-rotational mechanism after the saturated state, which results in a rather high coercivity field relative to the observed ones in real amorphous microwires with considerable larger lengths.

ACKNOWLEDGMENTS

I. Betancourt acknowledges the financial support from Research Grant IN106808 PAPIIT-UNAM, Mexico, as well as the supercomputing facilities of KanBalam, DGSCA-UNAM.

[1] A. Hernando and P. Marín, in *Concise Encyclopedia of Magnetic and Superconducting Materials*, 2nd ed., edited by K. H. J. Buschow (Elsevier, Amsterdam, 2005), p. 511.
[2] M. Vazquez, in *Handbook of Magnetism and Advanced Magnetic Materials*, edited by H. Kronmüller and S. Parking (Wiley, New York, 2007), Vol. 5, p. 2193.
[3] H. Chiriac and T. A. Óvari, in *Amorphous Wires and Glass-Covered Wires, Magnetic Amorphous Alloys: Structural, Magnetic and Transport Properties*, edited by P. Tiberto and F. Vinai (Research Signpost, Trivandum, 2003), p. 111.
[4] A. Zhukov and J. Gonzalez, in *Handbook of Advanced Magnetic Materials*, edited by Y. Liu, D. J. Sellmyer, and D. Shindo (Tsinghua University Press, Springer, New York, 2006), Vol. 3, p. 115.
[5] J. Fidler and T. Schrefl, J. Phys. D: Appl. Phys. **33**, R135 (2000).
[6] R. W. Chantrell, M. Wongsam, J. Fidler, and T. Schrefl, in *Micromagnetics: Finite Element Approach. Concise Encyclopedia of Magnetic and Superconducting Materials*, 2nd ed., edited by K. H. J. Buschow (Elsevier, Amsterdam, 2005), p. 928.
[7] D. R. Fredkin and T. R. Koehler, IEEE Trans. Magn. **26**, 415 (1990).
[8] T. R. Koehler, Physica B **233**, 302 (1997).
[9] G. Hrkac, T. Schrefl, O. Ertl, D. Suess, M. Kirschner, F. Dorfbauer, and J. Fidler, IEEE Trans. Magn. **41**, 3097 (2005).
[10] G. Hrkac, T. Schrefl, O. Ertl, D. Suess, M. Kirschner, F. Dorfbauer, and J. Fidler, J. Appl. Phys. **97**, 10E311 (2005).
[11] A. P. Zhukov, M. Vázquez, J. Velázquez, H. Chiriac, and V. Larin, J. Magn. Magn. Mater. **151**, 132 (1995).
[12] H. Chiriac, T. A. Óvári, and G. Pop, Phys. Rev. B **52**, 10104 (1995).
[13] J. Velázquez, M. Vázquez, and A. P. Zhukov, J. Mater. Res. **11**, 2499 (1996).
[14] P. Poulopoulos, S. Baskoutas, L. F. Kiss, L. Bujdosó, T. Kemény, F. Wilhelm, A. Rogalev, V. Kapaklis, C. Politis, M. Angelakeris, and K. Saksl, J. Non-Cryst. Solids **354**, 587 (2008).
[15] R. Alben, J. J. Becker, and M. C. Chi, J. Appl. Phys. **49**, 1653 (1978).
[16] G. Bertotti, E. Ferrara, F. Fiorillo, and P. Tiberto, Mater. Sci. Eng., A **226–228**, 603 (1997).
[17] R. C. O'Handley, *Modern Magnetic Materials* (Wiley, New York, 2000).
[18] V. Zhukova, N. A. Usov, A. Zhukov, and J. Gonzalez, Phys. Rev. B **65**, 134407 (2002).
[19] M. Vázquez and A. P. Zhukov, J. Magn. Magn. Mater. **160**, 223 (1996).
[20] M. Vázquez and A. Hernando, J. Phys. D: Appl. Phys. **29**, 939 (1996).